COMPUTATIONAL FLUID DYNAMICS ANALYSIS OF THE INFLUENCE OF INJECTION NOZZLE LATERAL OUTFLOW ON THE PERFORMANCE OF RANQUE-HILSCH VORTEX TUBE

by

Nader POURMAHMOUD [a]**, *Alireza IZADI*** [a]**, *Amir HASSANZADEH*** [b]*****,
and Ashkan JAHANGIRAMINI [a]

[a] Department of Mechanical Engineering, Urmia University, Urmia, Iran
[b] Department of Mechanical Engineering, College of Engineering, Mahabad Branch, Islamic Azad University, Mahabad, Iran

Original scientific paper
DOI: 10.2298/TSCI120704002P

In this article computational fluid dynamics analysis of a 3-D compressible and turbulent flow has been carried out through a vortex tube. The Standard k-ε turbulence model is utilized in order to simulate an axisymmetric computational domain. The numerical simulation has focused on the energy separation and flow field patterns of a somewhat non-conventional vortex tube, which is on the basis of creating an external hole at the end of each nozzle. According to the selected nozzles geometry, some of unfavorable phenomena such as shock wave, high pressure regions and appearing of unsymmetrical rotating flow patterns in the vortex chamber would be recovered significantly. In this way the physical parameters of flow field are derived under different both inlet mass flow rates and outlet pressures of nozzles hole. The results show that increasing outlet pressures of nozzles hole value enhanced the cooling capacity of machine in the most of operating conditions.

Key words: *vortex tube, computational fluid dynamics, energy separation, nozzles lateral outflow*

Introduction

Vortex tube or Ranque-Hilsch vortex tube is a mechanical device with a simple geometry, which is capable of splitting the entrance compressed flow into two different hot and cold streams. The compressed flow (arbitrary air) enters the tube tangentially through one or more nozzles. This instrument does not have any moving parts however generates two different hot and cold outlets. Each of these streams can be used according to the basic requirements. However the essential function of vortex tube is in cooling applications. The working fluid often used in vortex tube is compressed air. This device was invented accidentally many years ago by a French physicist Ranque [1] while he was conducting a research over vortex tube in the field of dust separation. A few years later, in 1945 German physicist Hilsch [2] worked on vortex tube consequently and developed main parameters of this system. He finally published the results of his work in an article in 1947. In fig. 1 a vortex tube and its components is displayed schematically. In recent years, the CFD techniques of fluid flow modeling and experimental investigations have been developed for more examination and clarification.

* Corresponding author; e-mail: amir.info@gmail.com

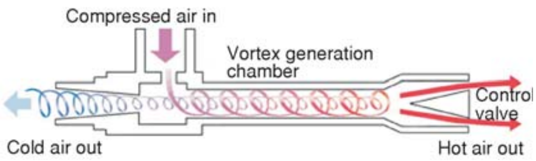

Figure 1. Schematic drawing of operational mechanism of a vortex tube

Takahama [3] investigated the geometrical parameters of the tube. Ahlborn and Gordon [4] studied the temperature separation in a low pressure vortex tube and stated that the separation is due to the secondary circulation. Saidi and Valipour [5] presented information data on the classification of the parameters affecting vortex tube operation. In their study, the thermo physical parameters such as inlet gas pressure, gas type and cold gas mass ratio, moisture of inlet gas and the geometrical parameters, *i. e*. diameter and length of main tube and area of the outlet orifice and shape of the entrance nozzle were designed and studied. Singh *et al*. [6] studied the vortex tube with different *L/D* ratio, nozzle size, cold orifice diameter and cold mass fraction. Behera *et al.* [7] used the 3-D CFD analysis to simulate the flow field and energy separation. Skye *et al*. [8] presented a comparison between the performance predicted by a 2-D computational fluid dynamic model and experimental measurements using a commercially vortex tube. Akhesmeh *et al*. [9] made a 3-D CFD model in order to study the variation of velocity, pressure, and temperature inside a vortex tube. Their results obtained upon numerical approach emphasized comprehensively on the mechanism of hot peripheral flow and a reversing cold inner core. Dincer *et al.* [10, 11] investigated the effect of control valve tip angle on the performance of Ranque-Hilsch vortex tube using different inlet pressures and different nozzle numbers and modeled the effects of length to diameter ratio and nozzle number on the performance of counter flow vortex tubes using artificial neural networks. Kirmaci [12] applied Taguchi method in order to optimize the number of nozzle of vortex tube and Kirmaci and Uluer [13] made an experimental investigation to determine the effects of inlet pressure on the heating and cooling performance of the counter flow vortex tube, by using air and oxygen as working fluid. Prabakaran and Vaidyanathan [14] researched the performance of a vortex tube with different diameters of nozzles and cold exit outlet. Bramo and Pourmahmoud [15] studied numerically the effect of length to diameter ratio (*L/D*) and importance of the stagnation point occurrence in flow patterns. Pourmahmoud *et al.* [16, 17] employed a full 3-D numerical simulation to study the effect of helical nozzles on the energy separation in the vortex tube and proposed an appropriate profile for this kind of nozzles by introducing a new dimensionless number, *i. e*. the radial gap of inlet of helical nozzle from the vortex chamber (GPL). Subsequently Pourmahmoud *et al.* [18] introduced the importance of the effect of inlet pressure on the performance of vortex tube by numerous numerical simulations. Since the nozzles set of a vortex tube plays the important role in the energy separation phenomenon, therefore any attempt in this field being considered as one of the top most researches.

Inserting the external hole at the end of nozzle where joined into the vortex chamber is the main goal of present research. Because at the relevant previous works, the increase of cooling capacity of a vortex tube merely were related to apply of types of nozzles (straight, helical, and convergent nozzles) or operating pressure and similar parameters. While occurring the unfavorable flow patterns in the vortex chamber can be regarded as a common problem. For example high inlet pressure in the straight nozzles may be useful in producing high rotating flow in the vortex chamber, but detailed analysis of flow filed shows the formation of shock wave layers; which dissipate the useful injected mechanical energy to the machine [18]. Controlling the flow field inside vortex chamber to reach a good level of cooling capacity will be possible under influence of generating a symmetrical rotating flow. Hence, the present article modifies the nozzles geometry at their external ends provides the exit of a few percent of additional inlet mass such that the appearance of shock waves and damping high pressure regions are recovered reasonably.

Governing equations

The compressible turbulent and highly rotating flow inside the vortex tube is assumed to be 3-D, steady-state and the Standard k-ε turbulence model is employed. The RNG k-ε turbulence model and more advanced turbulence models such as the Reynolds stress equations were also investigated, but these models could not be converged for this simulation [9]. Bramo and Pourmahmoud [15] showed that, because of good agreement of numerical results with the experimental data, the k-ε model can be selected to simulate the effect of turbulence inside the computational domain. Consequently, the governing equations are arranged by the conservation of mass, momentum, and energy equations together with equations for evaluating turbulence kinetic energy (k) and the rate of dissipation (ε). Theses equations have been presented previously in [9, 15-18] and they are not repeated here for brevity.

Physical modeling

The present created CFD model is based on that was used by Skye *et al*. [8]. It is noteworthy that, an ExairTM 708 slpm vortex tube was used by Skye to collect all of the experimental data. The dimensions of the model are available in the Skye *et al.* [8]. As described before, the present numerical simulation follows into taken to account of presence of an outflow hole at the end of injection nozzles to improve suitable flow patterns in order to increase of the cooling capacity of vortex tube. A schematic representation of the position of holes at the end of nozzles and their CFD models have been shown in fig. 2(a) and 2(b), respectively.

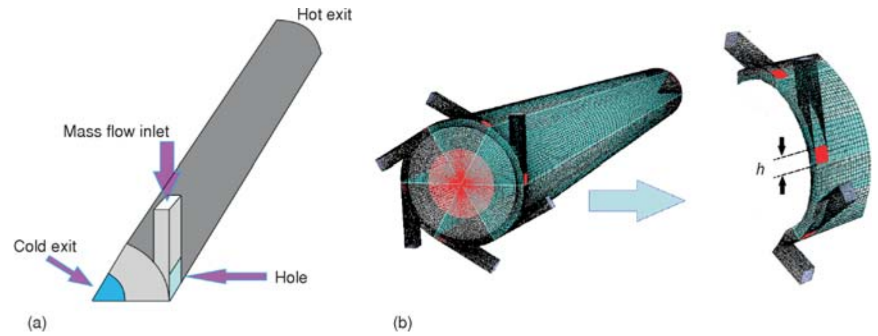

Figure 2. (a) A portrait of the position of square cross-section holes at the end of injection nozzles; (b) Corresponding 3-D CFD model of vortex tube with holed nozzles

These dimensions of nozzles hole are initial proposed values at the present paper, although the shape of holes or their dimensions can be investigated separately. Nevertheless, the intent of inserting an outflow place on the nozzles is to recover a vortex tube cooling capacity is the main goal of this article in spite of existence of many further discussions and investigations on the choosing of holes dimensional parameters in the future.

The considered nozzles hole have a square cross-section with a dimension of $h = 0.97$ mm, which is identical to nozzles height.

Boundary conditions for the models are determined based on the experimental measurements by Skye *et al.* [8]. The inlet is modeled as a mass flow inlet. The specified total mass flow rate and stagnation temperature are fixed to 8.35 g/s and 294.2 K, respectively. The static pressure at the cold exit boundary is fixed to experimental measurements pressure that is 0.15 bar *i. e.* fixed pressure outlet. The static pressure at the hot exit boundary is adjusted in the way to vary the cold mass fraction *i. e.* various pressure outlet. The same boundary condition is adjusted to the holes like hot outlet in order to set the amount of gas mass exiting from the holes. Another boundary condition which can be used for hot outlet and nozzles hole is by extending the outlet region and modeling the immediate ambient with pressure far-field boundary condition. In this paper a comparison for CFD model was done for two different boundary conditions of pressure outlet and pressure far-field. In all of quantitative and qualitative comparisons, there are not seen any considerable differences. So the pressure outlet boundary condition is used for hot outlet in this study. These results are summarized in the tab. 2. It must be mentioned that the results are obtained for special value of cold mass fraction $\alpha = 0.3$.

Table 1. Comparison between pressure outlet and pressure far-field boundary condition for hot outlet

Quantity	Pressure far-field	Pressure outlet	Difference [%]
T_c	250.85	250.24	0.243173
T_h	311.97	311.5	0.150656
$(Z/L)_v$	0.986	0.985	0.10142
T_{wmax}	310.714	310.119	0.191494
$(Z/L)_w$	0.834784	0.834784	0

In addition, a no-slip velocity boundary condition is enforced on all of the walls of vortex tube, and simultaneously they are assumed to be adiabatic.

The governing equations in the section *Governing equations* with k-ε turbulence model are analyzed by the FLUENT^{TM} software package. In order to discretize of derivative terms, the second order upwind and quick schemes are applied to momentum, turbulence, and energy equations. Bramo and Pourmahmoud [15] first showed that cold and hot exit temperature differences ($\Delta T_{i,c}$ and $\Delta T_{h,i}$) is predicted by the model and is in good agreement with the experimental values. The figures are not repeated here for brevity. Meanwhile, at a mass fraction about 0.3, the cold temperature differences can attain its maximum value.

Results and discussion

Effect of nozzles hole lateral outflow

The consequences of literature review confirm the issue of shock wave layers and unfavorable high pressure regions in the vortex chamber even at the best condition of cold mass fraction rate ($\alpha = 0.3$) and properly values of inlet pressure [18]. In order to clarification, fig. 3(a) represents the CFD numerical results of the pressure contours distribution in the vortex chamber for the Skye *et al*. [8] tested machine, which could help to realize the flow field structure precisely. It would be better to couple the behavior of compressible working fluid with the formation of Mach number levels, fig. 3(b). The generation of shock layer and high pressure zones are cleared at the end of injection nozzles, where they are jointed to vortex chamber where it is expected to attain a high rotating flow.

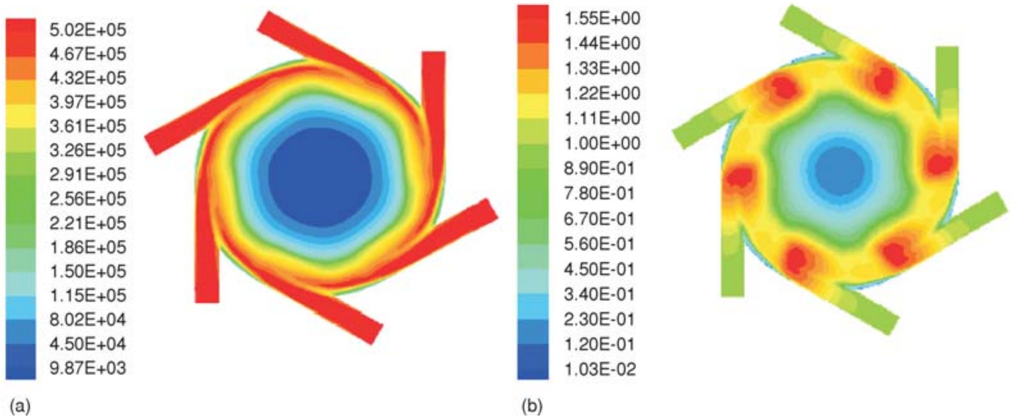

Figure 3. (a) Pressure contours in the vortex chamber; (b) Mach number contours in the vortex chamber, α = 0.3

Numerical results are evaluated based on 5 different outlet pressures of nozzles hole (OPH) including 0.1, 0.2, 0.3, 0.4, and 0.5 bar and 12 different $\dot{m}_{\text{in}}$ (6.24, 6.72, 7.26, 7.8, 8.34, 8.82, 9.18, 9.72, 10.26, 10.86, 11.52, and 12 g/s). The amount of outflow mass from each hole is very little in comparison with $\dot{m}_{\text{in}}$, such that the maximum mass exit from the holes is only 9% of total injected air; which corresponds to OPH = = 0.1 bar (fig. 4). The other question is arisen for operating of vortex tube due to apply of any $\dot{m}_{\text{in}}$ and OPH. The diagram of fig. 4 adequately answers to this issue. One gets that at OPH = = 0.1 bar, the vortex tube works for every $\dot{m}_{\text{in}}$; however OPH = 0.2 bar cannot form any flow regime for the first two values of $\dot{m}_{\text{in}}$ = 6.24 and 6.72 g/s.

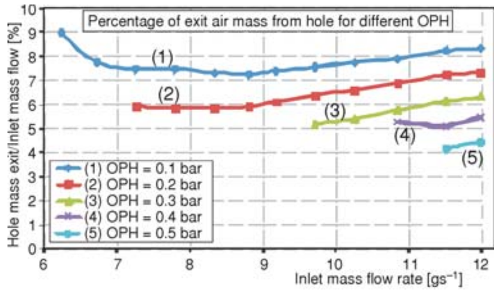

Figure 4. The percentage of mass flow rate exit from holes due to different hole pressures, α = 0.3

As ever the pressure of nozzles hole, *i. e*. OPH, is increased; the less amount of additional mass can be escaped form injection process. In contrast, the numbers of cases which vortex tube will be able to operate appropriately under higher OPH conditions become more confined. The reason of this phenomenon is the creation of a strong reversed flow near about the cold exit end.

Figure 5 shows the reversed flow at cold exit. Since the CFD model predicts that reversed flow will occur at the cold exit. While the occurring this problem, the flow comes back to the inlet region of the tube and it causes to increase of cold exit temperature which is not desired. So each case that creates the reversed flow is removed in this investigation. The results show that by increasing the OPH, the

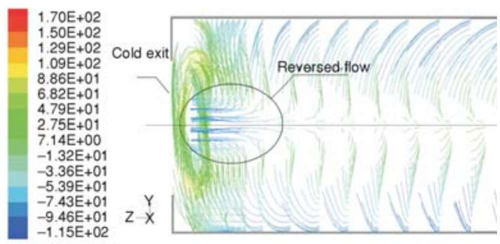

Figure 5. Generated reversed flow at the cold exit end region due to OPH = 0.5, $\dot{m}_{\text{in}}$ = 10 g/s, α = 0.3

number of cases that yield to creation of reversed flow are increased such that for OPH = 0.5 bar, only two data can be extracted from the numerical evaluation which are $\dot{m}_{\mathrm{in}} = 11.52$ and 12 g/s.

In order to have an appropriate insight of holes imposed to the injection nozzles and their effects (*e. g*. thermal performance) one has to compare the cold and hot exit temperatures for both situations of creating either hole or not. Pourmahmoud *et al.* [18] investigated the vortex tubes without outflow holes for different inlet mass flow rates. Figure 6 describes the cold exit temperatures for various hole pressures and compares them with the results of Pourmahmoud *et al.* [18]. It is revealed that, the cold exit temperature decreases by increasing OPH value even at high inlet mass flow rates. In addition, the trend of each curve represents descending rate for every OPH. Also, one can see that for every inlet mass flow rate the nozzles hole helped to drop of cold exit temperature except than 8.34 g/s (Skye *et al*. [8] experimental test).

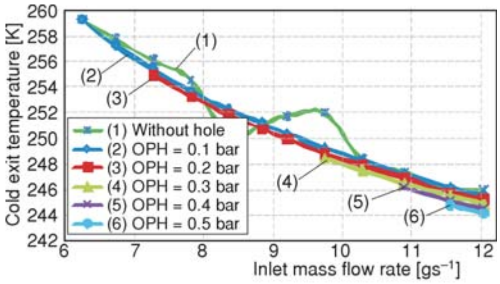

Figure 6. Cold exit temperature for different OPH and mass flow rate, α = 0.3

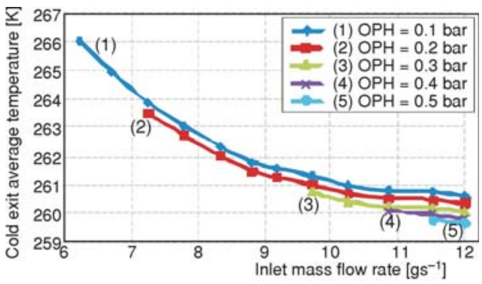

Figure 7. Averaged cold exit temperature for different OPH and mass flow rate, α = 0.3

A vortex tube when its nozzles is holed, would be suitable in order to operate throughout a wide range of inlet mass instead of fabricating a specific machine correspond to a definite input compressed gas. Indeed this idea would be useful for using a vortex tube due to any inlet mass flow rate if lateral outflow of nozzles hole drains some of additional injected mass. Figure 7 illustrates the averaged cold exit temperatures for different OPH. The same types of results can be obtained, however; the averaged values are somewhat greater than the minimum cold exit temperatures.

These cold exit temperature difference ($\Delta T_{\mathrm{i,c}}$) are summarized in tab. 3. The symbol '–' in a cell shows the creation of reversed flow for that case. The table tells some restrictions of lateral outflow idea. Because in many cases as mentioned before, the undesirable reversed flow phenomenon occurs in the cold exit end region which is a destructive mechanism for breaking regular cold mass producing. The hot exit temperature for different inlet mass flow rates and OPH has been shown in fig. 8. The result shows the improvement of hot exit temperature when the holes are created at the end of nozzles. For OPH = 0.1, 0.2 and 0.3, the hot exit temperature decreases as OPH rises. It is important to note that, there are not any significant distinctions among them.

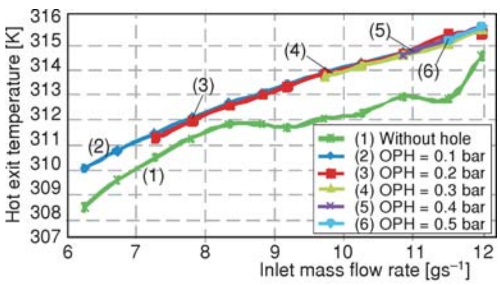

Figure 8. Hot exit temperature for different OPH and mass flow rate, α = 0.3

Table 3. Cold exit temperature difference for various OPH and inlet mass flow rates, α = 0.3

Mass flow rate [gs^{-1}]	Without hole	OPH = 0.1 bar	OPH = 0.2 bar	OPH = 0.3 bar	OPH = 0.4 bar	OPH = 0.5 bar
6.24	34.9498	34.959	–	–	–	–
6.72	36.46	36.9532	–	–	–	–
7.26	38.1388	38.8103	39.3021	–	–	–
7.80	39.6443	40.5033	40.9677	–	–	–
8.34	43.96	41.9184	42.3693	–	–	–
8.82	43.0701	42.9642	43.4057	–	–	–
9.18	42.4652	43.773	44.2222	–	–	–
9.72	42.171	44.8819	45.3037	45.6796	–	–
10.26	45.75	45.8229	46.2144	46.603	–	–
10.86	46.75	46.8428	47.1985	47.5799	47.9541	
11.52	48.058	47.8897	48.2974	48.5731	48.9886	49.2968
12	48.17	48.5407	48.8581	49.1924	49.5708	49.9152

However, as it was cited before, the vortex tube is often used for cooling applications not heating, so the cold exit temperature data are more important rather than hot exit temperature. Figure 9 also illustrates the average of hot exit temperatures for different OPH, which show that hot exit average temperatures are lower than maximum exit temperatures again. To realize the complete effect of nozzles hole influence on the flow field behavior, the contours of pressure for a specific inlet mass flow rate, 8.34 g/s, OPH = 0.1 and 0.2 bar are evaluated in vortex chamber. In fig. 10 these results demonstrate the confinement of high pressure regions as lateral outflow is passing through the nozzles hole, figs. 10(b) and 10(c).

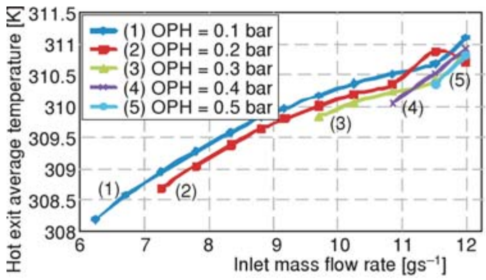

Figure 9. Average hot exit temperature for different OPH and mass flow rate, α = 0.3

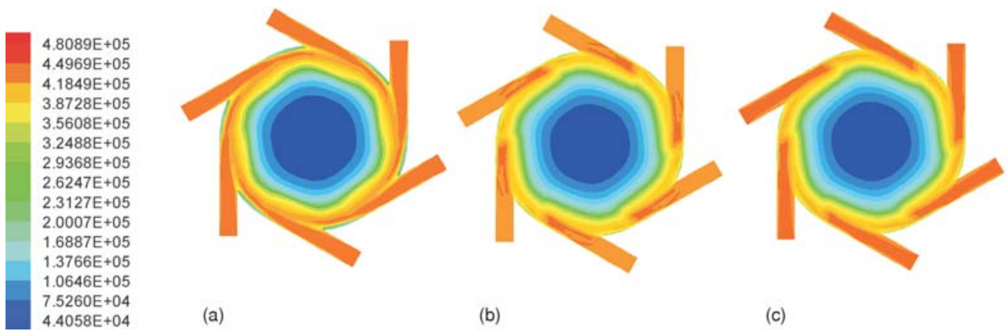

Figure 10. Pressure contour distribution in vortex chamber for $\dot{m}_{in}$ = 8.34 g/s; (a) without hole, (b) OPH = 0.1 bar, (c) OPH = 0.2 bar, α = 0.3

In the same manner, the existence of nozzles hole can be regarded as a mechanism that declares decreasing the effective area of high Mach number core at the exit of nozzles and hence decrease the possibility of shock waves occurrence. According to fig. 11, the Mach number distribution in the vortex chamber confirms the reduction of shock wave layers. The effect of nozzles hole can be analyzed by the other additional ways such as investigation of temperature distribution contours. It is obvious that lateral outflow of nozzles hole help to formation of suitable flow patterns such that the highly rotating flow in the chamber attains to its maximum possible value. Thus, the expectation of removing unfavorable flow field is somewhat satisfied; which leads finally to reduce the cold exit temperature.

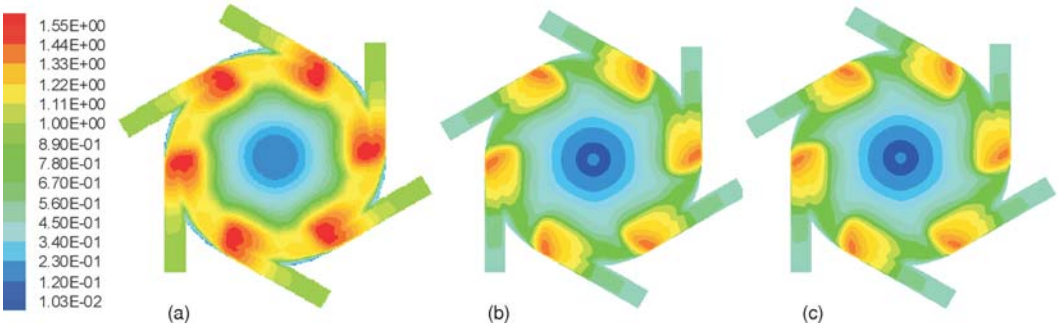

Figure 11. Mach number contour distribution in vortex chamber for $\dot{m}_{in}$ = 8.34 g/s; (a) without hole, (b) OPH = 0.1 bar, (c) OPH = 0.2 bar, α = 0.3

The obtained total temperature distribution contours are portrayed in fig. 12, which represent the peripheral flow to be warmer and core flow cooler respect to inlet temperature (294.2 K). Under operating condition of 8.34 g/s, maximum hot gas temperature of 311.5 K and minimum cold gas temperature of 250.24 K is produced for a vortex tube without hole. However, when the OPH is set to 0.2 bar along with inlet mass flow rate 8.34 g/s, then the clod and hot exit temperatures reach to 251.83 K and 312.25 K, respectively. According to two types of presented temperature distribution contours, the structures of contours for two models are al-

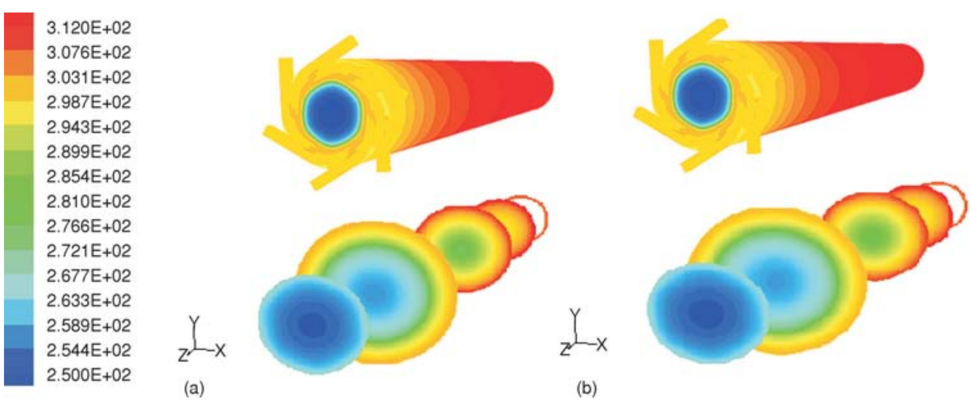

Figure 12. Temperature distribution contours in the vortex tube with 8.34 g/s inlet mass flow rate; (a) without hole, (b) OPH = 0.2 bar, α = 0.3

most the same; but there is a little difference between the lower and higher ranges of temperature levels.

In addition, the flow patterns as path lines at sectional lengths near the cold, hot exits and mid region are shown in fig. 13. The formation of core and peripheral streamlines can be clearly seen at the near cold end and mid region, but after occurring of separation phenomenon the core vortex is disappeared. In spite of creating of such reversed flow, the peripheral flow does not alter its continuation towards the hot end. One should notice that, the axial distance between stagnation point and hot exit end is too short. The path lines help to realize the flow patterns, so that any flow filed symmetry, various regions of hot and cold flow can be identified using them. Approaching to a properly symmetric rotating flow and effective intensively domain can be seen in fig. 13(a).

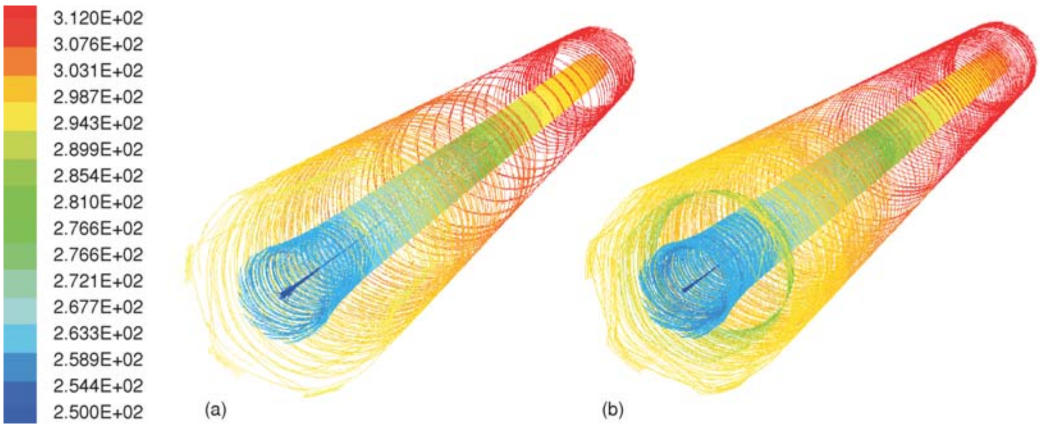

Figure 13. 3-D PATH lines colored by total temperature along the vortex tube with 8.34 g/s inlet mass flow rate; (a) without hole, (b) OPH = 0.2 bar, α = 0

Power separation analysis

The thermodynamical evaluation of the rate of power (energy) separation can be taken to account as another manner in order to analysis of either cooling or heating capacity of a vortex tube. The symbols $\dot{Q}_c$ and $\dot{Q}_h$ represent the rate of energy separation in the hot and cold exit streams and they are determined numerically. The relevant formulations are given as:

$$\dot{Q}_c = \dot{m}_c c_p (T_{in} - T_c) \tag{1}$$

$$\dot{Q}_h = \dot{m}_h c_p (T_h - T_{in}) \tag{2}$$

The values of $\dot{Q}_c$ and $\dot{Q}_h$ are summarized in figs. 14 and 15, where the cold mass fraction is kept about 0.3.

The $\dot{Q}_c$ for the vortex tube varies from 0.22 to 0.58 kW for OPH = 0.1 bar, while this range alters from 0.097 to 0.26 kW for $\dot{Q}_h$, accordingly. One has to note that, the curves of energy separation coincide to each other for any OPH, whether heating or cooling. Hence, it would be inferred that in the vortex tube system, the main goal should be focused on the using this machine in the local heating or cooling process only. Therefore, the classical thermodynamics criteria would not be justified in many conditions. Thus, according to the last figures $\dot{Q}_c$ and $\dot{Q}_h$ curves are not sufficient to explore the task.

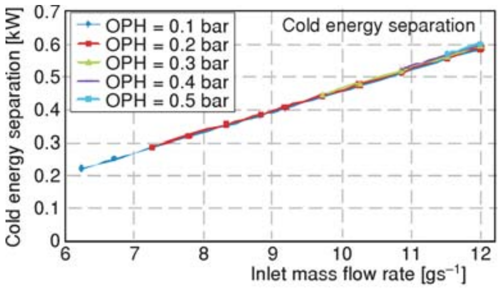

Figure 14. Comparison of cold power separation rate for different OPH, α = 0.3

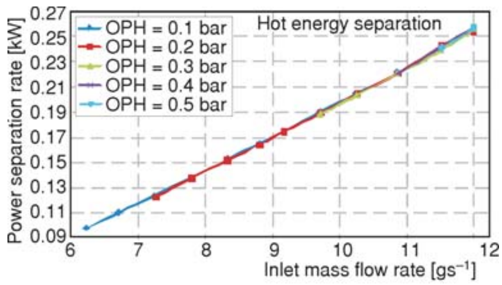

Figure 15. Comparison of hot power separation rate for different OPH, α = 0.3

Conclusions

In this article, a numerical investigation has been carried out to recover the performance of a somewhat non-conventional vortex tube. The main proposal of the present research is based on creating an external hole at the end of injection nozzles, where they are jointed to the vortex chamber. These nozzles configuration help to employ of a vortex tube in the wide range of inlet mass flow rates not merely to a certain designed input compressed working flow. Simulation of various cases showed that only a few percent of additional inlet mass must be drained through holes, otherwise this mechanism leads to generate of reversed flow at the cold exit end. Adjusting the nozzles lateral outflow such that both injected and escaped flows from the holes have a meaningful correlation is the necessary condition in order to attain a good level of cooling capacity. The results of CFD models due to apply of various outlet pressure of nozzles hole (OPH) and different inlet mass flow rates are derived and analyzed from different points of view particularly analyzing the cold and hot exit temperature differences along with cold and hot power separations.

The obtained numerical results revealed that the equipped nozzles would be more efficient in removing destructive shock layers, high pressure regions and unsymmetrical rotating flow patterns through the vortex chamber. Hence, the low range of cooled exit temperature can be produced. In addition, the compatibility of some of the basic numerical results with the Skye *et al.* [8] experimental data shows the reasonable agreement on the studied issue.

Nomenclature

D	–	diameter of vortex tube, [mm]
h	–	nozzle height, [mm]
k	–	turbulence kinetic energy, [m^{2}s^{-2}]
L	–	length of vortex tube [mm]
$\dot{m}_{\mathrm{in}}$	–	inlet mass flow rates, [gs^{-1}]
OPH	–	outlet pressure of nozzles hole, [bar]
$\dot{Q}_{\mathrm{c}}$	–	cold exit separation rate, [kW]
$\dot{Q}_{\mathrm{h}}$	–	hot exit separation rate, [kW]
R	–	radial distance measured from the centerline of tube, [mm]
T	–	temperature, [K]
$\Delta T_{\mathrm{i,c}}$	–	cold exit temperature difference, [K]
$\Delta T_{\mathrm{i,h}}$	–	hot exit temperature difference, [K]
T_{wmax}	–	maximum wall temperature, [K]
w	–	nozzle width, [mm]
$(Z/L)_{\mathrm{w}}$	–	axial location of maximum wall temperature
$(Z/L)_{\mathrm{v}}$	–	axial location of stagnation point

Greek symbols

α	–	cold mass fraction, [–]
ε	–	turbulence dissipation rate, [m^{2}s^{-3}]
μ	–	dynamic viscosity, [kgm^{-1}s^{-1}]
μ_{t}	–	turbulent viscosity [kgm^{-1}s^{-1}]
ρ	–	density, [kgm^{-3}]
σ	–	stress, [Nm^{-2}]
τ	–	shear stress, [Nm^{-2}]
τ_{ij}	–	stress tensor components, [Nm^{-2}]

References

[1] Ranque, G. J., Experiences on Expansion in a Vortex with Simultaneous Exhaust of Hot Air and Cold Air (in French), *J. Phys.Radium, 4* (1933), 7, pp. 112-114
[2] Hilsch, R., The Use of Expansion of Gases in Centrifugal Field as a Cooling Process (in German), *Z. Naturforschung, 1* (1946), Feb., pp. 208-214
[3] Takahama, H., Studies on Vortex Tube, *Bull. JSME, 8* (1965), pp. 433-440
[4] Ahlborn, B., Gordon, J., The Vortex Tube as a Classical Thermodynamic Refrigeration Cycle, *J. Applied Phys., 88* (2000), 6, pp. 645-653
[5] Saidi, M. H., Valipour, M. S., Experimental Modeling of Vortex Tube Refrigerator, *App. Therm. Eng. 23* (2003), pp. 1971-1980
[6] Singh, P. K., *et al.*, An Experimental Performance Evaluation of Vortex Tube, *IE (I) Journal.MC, 84* (2004), pp. 149-153
[7] Behera, U., *et al.*, CFD Analysis and Experimental Investigations Towards Optimizing the Parameters of Ranque-Hilsch Vortex Tube, *Int. J. Heat and Mass Trans., 48* (2005), 10, pp. 1961-1973
[8] Skye, H. M., *et al*., Comparison of CFD Analysis to Empirical Data in a Commercial Vortex Tube, *Int. J. Refrigeration, 29* (2006), 1, pp. 71-80
[9] Akhesmeh, S., *et al*., Numerical Study of the Temperature Separation in the Ranque-Hilsch Vortex Tube, *Am. J. Eng. Appl. Sci., 1* (2008), 3, pp. 181-187
[10] Dincer, K., *et al.*, Modeling of the Effects of Length to Diameter Ratio and Nozzle Number on the Performance of Counter Flow Ranque-Hilsch Vortex Tubes Using Artificial Neural Networks, *Appl. Therm. Eng., 28* (2008), pp. 2380-2390
[11] Dincer, K., *et al*., Experimental Investigation of the Performance of a Ranque-Hilsch Vortex Tube with Regard to a Plug Located at the Hot Outlet, *Int. J. Refrigeration, 32* (2009), pp. 87-94
[12] Kirmaci, V., Optimization of Counter Flow Ranque-Hilsch Vortex Tube Performance Using Taguchi Method, *Int. J. Refrigeration, 32* (2009), 6, pp. 1487-1494
[13] Kirmaci, V., Uluer, O., An Experimental Investigation of the Cold Mass Fraction, Nozzle Number, and Inlet Pressure Effects on Performance of Counter Flow Vortex Tube, *J. Heat Trans., 131* (2009), 8, pp. 603-609
[14] Prabakaran, J., Vaidyanathan, S., Effect of Diameter of Orifice and Nozzle on the Performance of Counter Flow Vortex Tube, *Int. J. Eng. Sci. and Tech., 2* (2010), 4, pp. 704-707
[15] Bramo, A. R., Pourmahmoud, N., Computational Fluid Dynamics Simulation of Length to Diameter Ratio Effect on the Energy Separation in a Vortex Tube, *Thermal Science, 15* (2011), 3, pp. 833-848
[16] Pourmahmoud, N., *et al*., Computational Fluid Dynamics Analysis of Helical Nozzles Effects on the Energy Separation in a Vortex Tube, *Thermal Science, 16* (2012), 1, pp. 151-166
[17] Pourmahmoud, N., *et al*., Numerical Analysis of the Effect of Helical Nozzles Gap on the Cooling Capacity of Ranque-Hilsch Vortex Tube, *Int. J. Refrigeration, 35* (2012), 5, pp. 1473-1483
[18] Pourmahmoud, N., *et al*., Numerical Investigation of Operating Pressure Effects on the Performance of a Vortex Tube, *Thermal Science, 18* (2014), 3, pp. 1191-1201

Paper submitted: July 4, 2012
Paper revised: December 14, 2012
Paper accepted: January 3, 2013